Supporting Information

For

Nanoscale 3D Chiral Plasmonic Helices with Circular Dichroism at Visible Frequencies

Marco Esposito[1], Vittorianna Tasco[1], Massimo Cuscunà[1], Francesco Todisco[1], Alessio Benedetti[2], Iolena Tarantini[3], Milena De Giorgi[1], Daniele Sanvitto[1] and Adriana Passaseo[1].*

1- National Nanotechnology Laboratory (NNL), Istituto Nanoscienze, CNR, via Arnesano, I-73100 Lecce, Italy

2- Università di Roma La Sapienza, Dip. SBAI, Via Scarpa 16, 00161 Roma, Italy

3- Università del Salento, Dip. Mat-Fis Ennio De Giorgi, I-73100 Lecce, Italy

E-mail: marco.esposito@nano.cnr.it

Shape dependence of the beam parameters

In figure S1a we show the evolution of 3D FIBID nanohelices at different dose values as a function of the step size and constant ion energy (30 keV). Since the dose, as known, depends on step size and dwell time, for the same value of the step size, a variation of the dose directly reflects a dwell time change.

As the increased dwell time leads to an increased amount of deposited material, expanding the volume of each spot and allowing a better overlap between consecutive spots, the step size threshold moves toward larger values with a nearly linear dependence (red circles in figure S1a) on the dose resulting also in a wide range of VP control, from 200 nm to 2000 nm. In addition, keeping

constant the beam parameters and the dose value (100 pC/μm), we observed a slight increase in the obtained wire diameter with the increase of the step size, promoted by the built up dwell time of the smaller spot number (figure S2). Optimal control for nanohelix grown by the focused ion beam was reached with the minimum current value achievable by the instrument, 1 pA, at 30 keV as accelerating voltage, and setting a step size of 10 nm.

Figure S1b shows that, even for FEBID, despite the current used is 17 times higher, the step size threshold is lower for low dose values, due to the reduced beam diameter. Dose escalation moves only slightly the threshold to higher values with increasing dwell time. On the other hand, maintaining a constant dose and increasing the step size, the spots are well spaced out with poor enlargement of the diameter and a remarkable growth in height. So, as compared to the FIBID case, the expansion of the WD turns out to be negligible while the obtained VP is far higher.

Moreover, despite a higher current is employed with respect to the ion beam case, in FEBID we still needed to compensate the lower precursor ionization efficiency of the electron beam, by adequately increasing the dwell time (total dose),[1-3] to achieve the same VP flexibility degree of the FEBID. Such a correction, however, must be limited, since a too large dwell time value would lead to a reduction of the volume per dose due to a greater material depletion in the growth area.

Following this investigation, for FEBID nanohelices, the minimum probe size and a high deposited volume localization[4] were found with a current of 17 pA (corresponding to aperture diameter of 10 μm) and 10 keV as accelerating voltage.

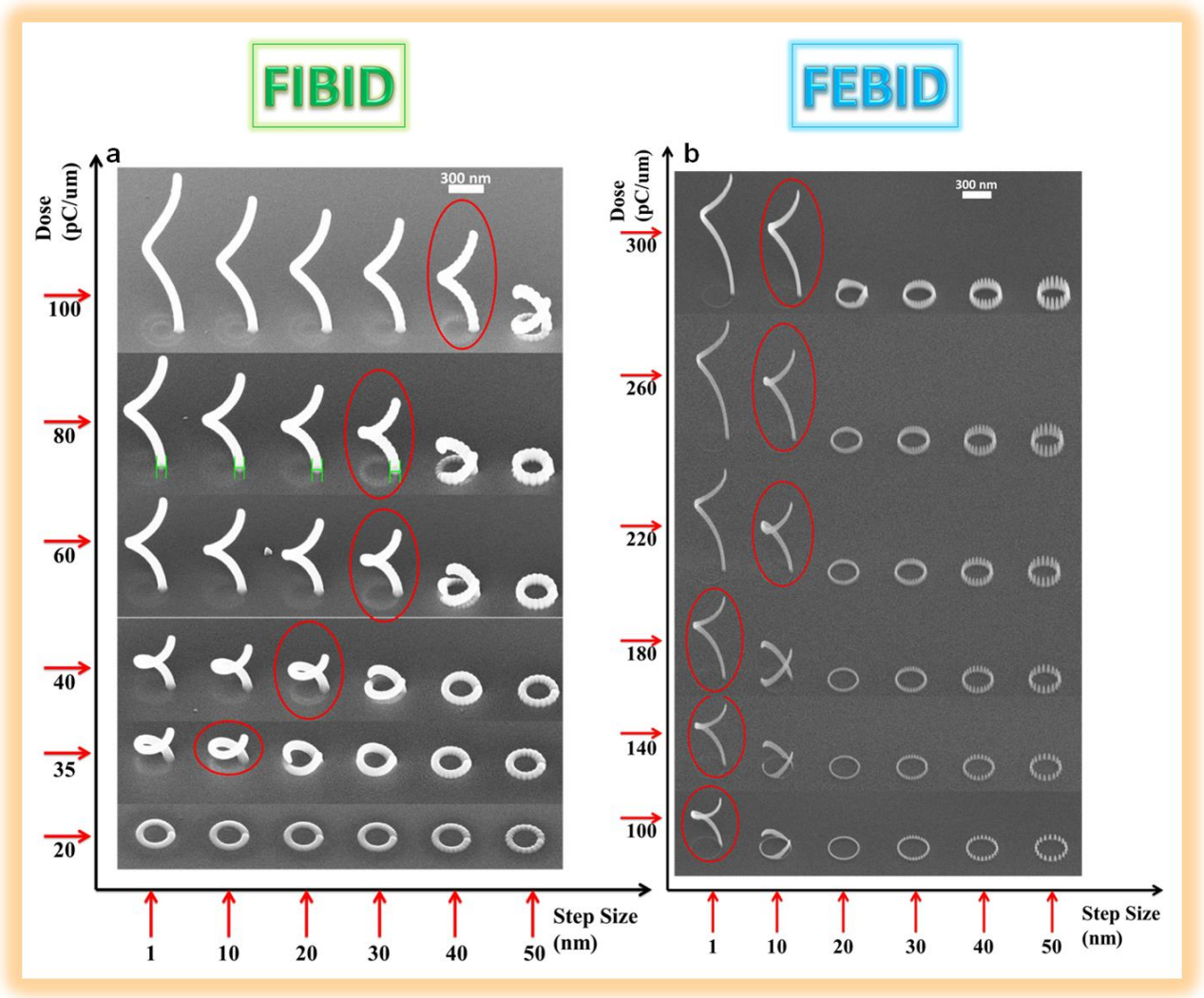

Figure S1. *a) Evolution of 3D FIBID nanohelices at different dose values (dwell time) as a function of the step size. The current and the acceleration voltage were kept constant, respectively at 1 pA and 30 keV. b) 3D FEBID nanohelices fabricated at different dose as a function of the step size. The current and the acceleration voltage were kept constant, respectively at 17 pA and 10 keV. For each constant dose value for step size values higher than the threshold, the spots remain spaced with a slight broadening of the diameter and greater increase in height.*

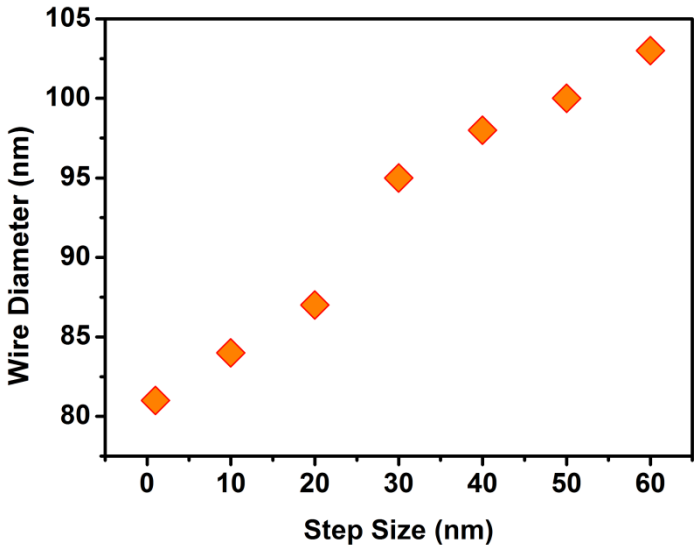

***Figure S2**. Measured FIBID nanohelix wire diameter as a function of the step size.*

LCP and RCP Reflection spectra

Reflectance spectra of the fabricated array (shown in figure 3b) were measured in a self-made confocal system coupled with an inverted optical microscope, using a 40x objective lens (NA 0.9) to collect light in a cone with 64° semi-aperture angle. Light reflected from the sample was spatially selected and focused on a CCD and the reflectance spectra were calculated with respect to the light reflected by a calibrated silver mirror.

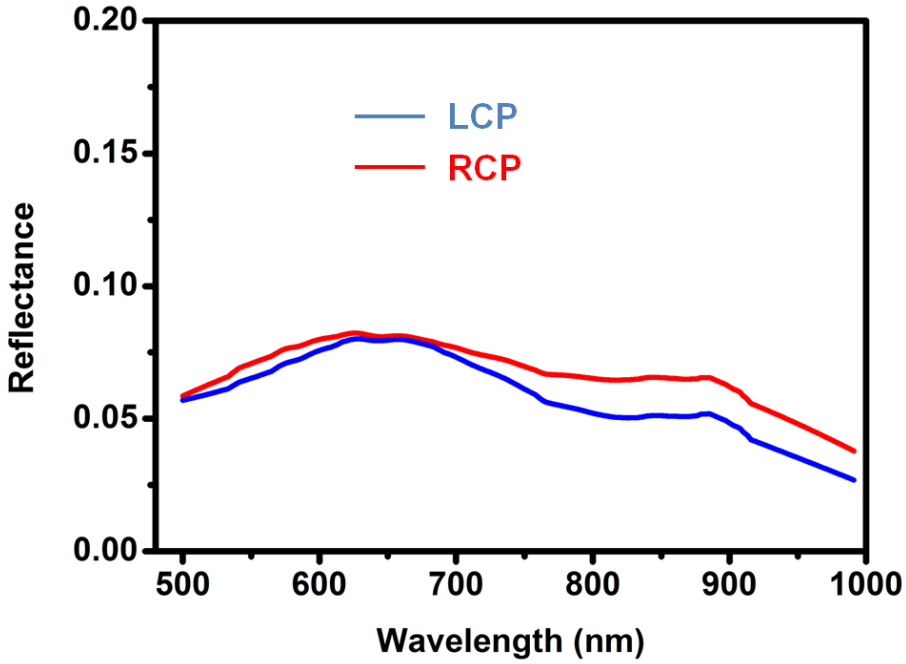

Figure S3. *Measured LCP and RCP reflection spectra for FIBID nanohelix array in the visible range.*

Circular dichroism control as a function of the nano-helix geometrical parameters

The circular dichroism band of nano-helix arrays realized by FIBID/FEBID can be modulated in the VIS/NIR by varying the geometrical parameters of the nanostructures in a subwavelength regime. Figure S4 shows the dissymmetry factor behavior for different sets of structural parameters. It can be noted that the dichroic band of FIBID nano-helices is wide for all combinations of nanostructure sizes. A high selectivity and a large blue-shift of the dichroic band can only be achieved with the smaller nanohelices realized by FEBID (sample 5).

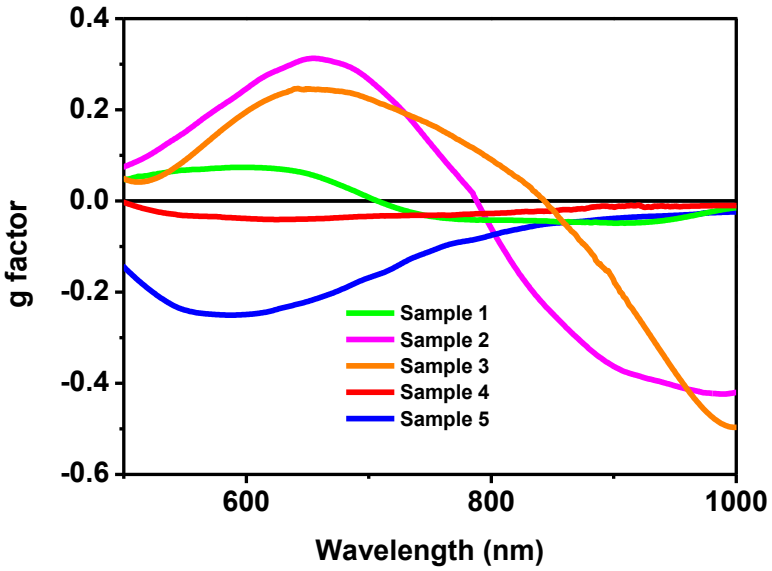

***Figure S4**. Measured g factor for FIBID and FEBID nanohelices with different geometric parameters except the lattice parameters kept at 700 nm for all the FIBID samples and 400 nm for the FEBID sample. Sample 1 (green line): g factor of 1 loop FIBID nano-helix array with ED=330 nm, VP=190 nm, WD=80 nm; Sample 2 (magenta line): g factor of 3 loop FIBID nano-helix array with ED=400 nm, VP=300 nm, WD=130 nm; Sample 3 (orange line): g factor of 5 loop FIBID nano-helix array with ED=300 nm, VP=210 nm, WD=130 nm. Sample 4 (red line): g factor of 1 loop FIBID nano-helix array with ED=200 nm, VP=120 nm, WD=80 nm. Sample 5 (blue line): g factor of 3 loop FEBID nano-helix array with ED=215 nm, VP=350 nm, WD=60 nm.*

Dispersion curves of the Pt/C mixture

The refractive index spectra have been calculated by adopting the dispersions for the refractive indexes of Pt and C both retrieved from ref 5, using the Maxwell-Garnett formula[6] for the effective medium approximation, and finally assuming a variable percentage of the two basic constituents into the composite material, inverting the guest/host attributes according to the selected percentage. In general terms, the Maxwell Garnett approach is expected to be highly accurate for low percentages of inclusions, since it is requested that the guest domains are spatially separated into the host environment. Anyway, it still maintains validity for higher volume fractions of the inclusions, and it is generally assumed as the most accurate tool to get sufficiently accurate estimates for the resulting effective medium.

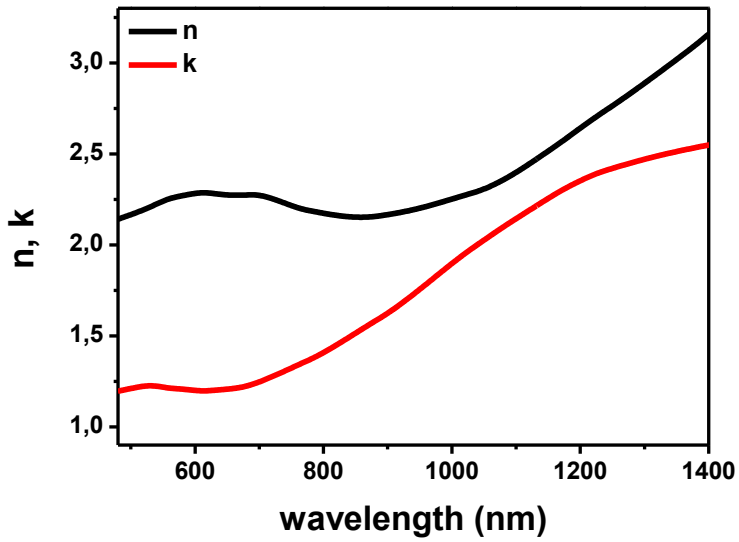

Figure S5: *The calculated refractive index spectra of the Pt-C alloy.*

Fabrication tolerances and their effect on the transmission spectra

A theoretical evaluation of transmission spectra evolution as a function of geometrical size variation within the fabrication tolerance range was also performed. In agreement with previous studies,[7,8] the stronger effect seems induced by the ED variation, where a 10% decrease (increase), while leaving unchanged the other parameters, leads to a blue- (red-) shift of the resonance peaks of 30 nm (figure S6a). On the other hand, an increase (decrease) of 10% of the VP value, corresponds to a minor blue- (red-) shift of the RCP resonance in the transmissions spectra (figure S6b).

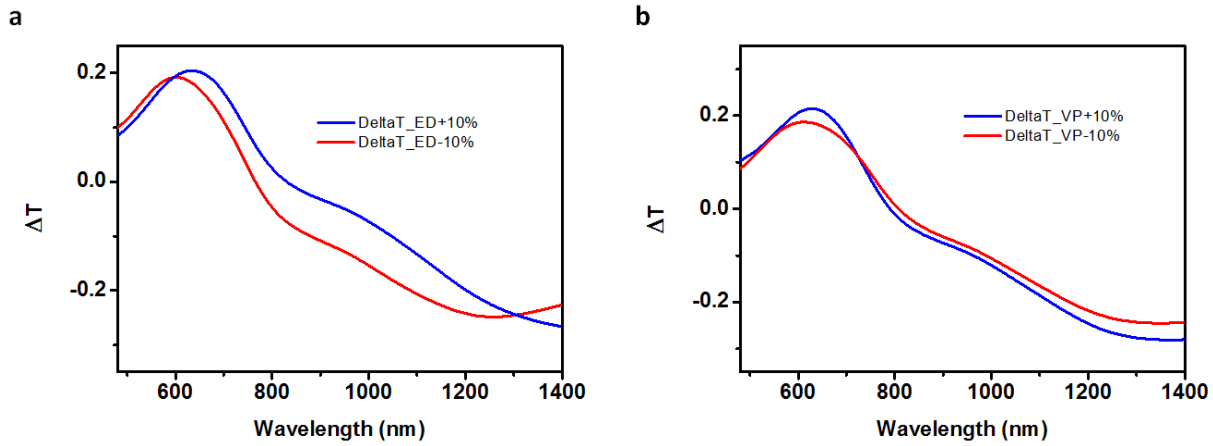

Figure S6: *Calculated transmission difference spectra obtained by considering a) the ED value of ±10% and b) the VP value of ±10% with respect to the average values of 400 nm for ED and 300 nm for VP of the FIBID array.*

Supporting Information References

1. Fowlkes, J. D.; Rack, P. D. Fundamental Electron-Precursor-Solid Interactions Derived from Time-Dependent Electron-Beam-Induced Deposition Simulations and Experiments. *ACS Nano*, **2010**, *4*, 1619–1629.

2. Serrano-Ramón, L.; Córdoba, R.; Rodríguez, L. A.; Magén, C.; Snoeck, E.; Gatel, C.; Serrano, I.; Ibarra, M. R.; De Teresa, J. M. Ultrasmall Functional Ferromagnetic Nanostructures Grown by Focused Electron-Beam-Induced Deposition. *ACS Nano*, **2011**, *5*, 7781–7787.

3. Beaulieu, D.; Ding, Y.; Wang, Z. L.; Lackey, W. J. Influence of Process Variables on Electron Beam Chemical Vapor Deposition of Platinum. *J. Vac. Sci. Technol. B* **2005***, 23*, 2151-2159.

4. Lipp, S.; Frey, L.; Lehrer, C.; Demm, E.; Pauthner, S.; Ryssel, H. A Comparison of Focused Ion Beam and Electron Beam Induced Deposition Processes. *Microelectron. Reliab.* **1996**, *36,* 1779-1782.

5. Palik, E. D. Handbook of Optical Constants of Solids. Academic Press **1991**.

6. Maxwell, G. J. C. Colours in Metal Glasses and Metal Films. *Phil. Trans. R. Soc. London A* **1904,** *3*, 385–420.

7. Gansel, J. K.; Wegener, M.; Burger, S.; Linden, S. Gold Helix Photonic Metamaterials: A Numerical Parameter Study. *Optics Express* **2010**, *18*, 1059-1069.

8. Yang, Z. Y.; Zhao, M.; Lu, P. X. A Numerical Study on Helix Nanowire Metamaterials as Optical Circular Polarizers in the Visible Region. *Photonics Technology Letters, IEEE* **2010**, *22,* 1303-1305.